J Mater Sci (2012) 47:7167–7174
DOI 10.1007/s10853-012-6659-9

Effect of different aqueous synthesis parameters on the size of CdSe nanocrystals

H. Etxeberria · G. Kortaberria · I. Zalakain · A. Larrañaga · I. Mondragon

Received: 10 February 2012 / Accepted: 10 June 2012 / Published online: 30 June 2012

Abstract The variation of CdSe nanoparticle size as a function of synthesis conditions is presented. Cadmium sulphate ($CdSO_4$), cadmium chloride ($CdCl_2$) and sodium selenosulphate (Na_2SeSO_3) solutions were used as precursors. Nanoparticles were synthesized by aqueous chemical methods. The synthesis parameters studied were pH, Cd:Se ratio and the type of stabilizing agent. Three different stabilizing agents were used, thioglycolic acid, mercaptoethanol and poly(vinyl pyrrolidone). Fourier transform infrared spectroscopy results confirmed the presence of the stabilizing agent on the surface of the nanoparticles. Ultraviolet visible and X-ray powder diffraction measurements were used to estimate the trend of size variations of the particles with different synthesis parameters, which agreed fairly by both techniques and the crystal structure. Additionally, the size of the nanoparticles was obtained by transmission electron microscopy measurements. Whilst the effect of pH was different for each of the different stabilizing agents due to the different chemical groups in the thiol compounds and the size of the nanoparticles varied with the used stabilizing agents, the effect of Cd:Se ratio in the size of nanoparticles showed the same tendency for the several stabilizing agents.

H. Etxeberria · G. Kortaberria · I. Zalakain · I. Mondragon (✉)
Group 'Materials + Technologies', Escuela Politécnica, Department of Chemical & Environmental Engineering, Universidad País Vasco/Euskal Herriko Unibertsitatea, Pza. Europa 1, 20018 Donostia-San Sebastián, Spain
e-mail: galder.cortaberria@ehu.es

A. Larrañaga
Faculty of Science and Technology, General Research Services (SGIker), Universidad País Vasco/Euskal Herriko Unibertsitatea, P.O. Box 644, 48080 Bilbao, Spain

Introduction

Semiconductor nanoparticles (NP) have been the subject of intensive studies due to their size-dependent electronic and optical properties and their potential applications in biological labelling, microelectronics and optical communication [1–6]. There are two major effects in NP properties which are responsible for these size variations. Firstly, the number of surface atoms is a large fraction of the total and their contribution to the free energy is distinct to that of the inner ones. Secondly, the intrinsic properties of NP are transformed by quantum size effects [7]. When the size of the NP becomes comparable or less than the Bohr radius of the exciton, the electron hole pair, in the bulk material quantum confinement occurs, the energy band gap widens and the absorption edge shifts towards the high-energy side. The two existent general strategies of NP preparation are organometallic synthesis based on high-temperature thermolysis of the precursors (TOPO/TOP route) [8–14] or dehalosilylation reaction [15, 16], and on the other side the synthesis in aqueous medium using polyphosphates [17] or thiols [18–22] as stabilizing agents (arrested precipitation). TOPO–TOP route produces NP with very good properties, such as high photoluminescence (PL), quantum efficiency, narrow full width of half-maximum (FWHM) of PL spectra, excellent monodispersity and high photostability. However, these NPs are only soluble in some non-polar organic solvents, which makes them non useful for biological applications [23]. The NP which are created by arrested precipitation in aqueous media exhibit properties suitable for biolabelling applications. Some of the advantages of the aqueous synthesis are its simplicity and high reproducibility as well as the possibility of easily controlling the surface charge and other surface properties of thiol-capped NP by the choice of the stabilizing agent with

appropriate free functional groups [24]. Among the various kinds of semiconductor NP, colloidal CdSe NP are the most widely investigated because their emission can be easily tuned to cover from red to blue as their size decreases.

In this work, the effect of different stabilizing agents and diverse synthesis parameters on the particle size of CdSe NP synthesized by aqueous chemical methods was investigated characterizing the presence of each stabilizing agent on the surface of NP by Fourier transform infrared spectroscopy (FTIR) and studying the effect of the bond nature between NP and stabilizing agent by several techniques.

Experimental

Materials

Cadmiun sulphate hydrate ($3CdSO_4 \cdot 8H_2O$), selenium metal powder (Se) and sodium sulphite (Na_2SO_3) were purchased from Panreac. 2-mercaptoethanol (ME), thioglycolic acid (ThGA) stabilizing agents, cadmium chloride ($CdCl_2$), poly(vinyl pyrrolidone) (PVP) and methanol were supplied by Aldrich. All materials were used without further purification.

ME- and ThGA-capped CdSe particles

Na_2SeSO_3 aqueous solution was prepared freshly by dissolving Se powder in Na_2SO_3 solution under nitrogen atmosphere at 90 °C for 24 h. A 0.04 M solution of $CdSO_4$ was prepared by dissolving 0.51327 g of $3CdSO_4 \cdot 8H_2O$ in 50 mL of deionized water. Mercapto compound-coated NP aqueous solution was synthesized by adding freshly prepared Na_2SeSO_3 solution to nitrogen saturated $3CdSO_4 \cdot 8H_2O$ 0.04 M aqueous solutions at pH = 9 in the presence of thiol stabilizing agents [20]. The addition of Na_2SeSO_3 produced bright-yellow, transparent colloids stable towards oxidation under air. Different synthesis parameters, pH (7, 9, 11) and Cd/Se ratios (1/5, 1/2, 1, 2 and 5), were employed. Nanocrystal growth time was 1 h at all the different synthesis conditions.

PVP-capped CdSe NP

A 0.04 M aqueous solution of Na_2SeSO_3 was used. A 0.04 M $CdCl_2$ solution in methanol was also prepared. Different amounts of PVP were added to $CdCl_2$ solution in methanol and stirred vigorously. Addition of Na_2SeSO_3 to the $CdCl_2$ solution produced a yellow pale precipitant which turned to red. Water was kept out using rotavapor and, PVP-capped particles were redispersed in methanol.

pH adjustment

pH of $3CdSO_4 \cdot 8H_2O$ and stabilizing agent solution was adjusted by dropwise addition of 1 M NaOH. The fixed Cd/Se ratio during these syntheses was 2/1. In the case of PVP, as no effect of pH was observed there is no data shown.

Cd/Se ratio

The Cd/Se molar ratios were altered, whilst Cd/stabilizing agent ratio was kept constant (1/2 in the case of thiol stabilizing agents and 1/1.25 in the case of PVP). The Se concentration was fixed and Cd concentration was varied. The pH value during these syntheses was 9.

Characterization

FTIR spectra were carried out in a Nicolet Magna IR system 750 spectrometer. Spectra were taken with 2 cm^{-1} resolution in a wavenumber range from 4000 to 400 cm^{-1}. The NP were pressed in KBr to form pellets and dried under vacuum before measurements.

UV–Vis measurements were taken using a Jasco V-630 spectrophotometer. Optical absorption studies were carried out by dispersing nanoparticle powder in different solvents and using the respective solvent as the reference.

X-ray powder diffraction (XRD) patterns were collected using a Philips X-Pert automatic diffractometer operating at 40 kV and 40 mA in theta–theta configuration, secondary monochromator with Cu Kα radiation ($\lambda = 1.5418$ Å) and a PIXcel solid state detector. The samples were mounted on a zero background silicon wafer fixed in a generic sample holder. Data were collected from 10 to 70° 2θ (step size = 0.026 and time per step = 30 s) at room temperature. A fixed divergence and antiscattering slit giving a constant volume of sample illumination were used. Removal of the instrumental broadening was done collecting a pattern LaB_6 standard. The X-ray powder pattern of LaB6 standard was collected in the same diffractometer conditions; the obtained data were fitted by the Rietveld method using the FULLPROF program [25, 26]. The obtained instrumental resolution function for the LaB6 was used to calculate this contribution at 25.6 degrees (0.063°) to remove this value from the obtained FWHM of the (111) reflection of the CdSe phase.

The nanoparticle size was determined by transmission electron microscopy (TEM). A solution drop was deposited on a Formvard film Copper grid and examined in a Tecnai G2 20 Twin (FEI) microscope operating at an accelerating voltage of 200 keV in a bright-field image mode.

Results and discussion

FTIR spectroscopy

The adsorption to the nanoparticle surface of the different stabilizing agents was confirmed by FTIR spectroscopy. Representative spectra of the stabilizing agents and their coated NP are shown in Fig. 1a–c. In the case of the neat thiol material (Fig. 1a), a sharp peak for S–H stretching was observed at 2563 cm^{-1}. For the NP there was no S–H stretching band, which indicated that the H atom of the mercapto group was replaced by Cd. This fact confirmed the adsorption of the mercapto compounds on the surface of CdSe NP [27]. ThGA surface-coated NP exhibited an O–H stretching band at 3440 cm^{-1}, a COO– symmetrical stretching at 1570 cm^{-1} and a COO– unsymmetrical stretching at 1380 cm^{-1}, which were induced by the cadmium–thiolate complexes covalently bound to the CdSe NP [28].

On the other hand, for ME–CdSe NP (Fig. 1b), ME–OH group stretching and $-CH_2$ bending vibrations were, respectively, observed in the ranges of 3400 and 1419 cm^{-1}. Furthermore, C–O primary stretching bands at 1042 and 1007 cm^{-1} were also identified. Most of the bands showed a red shift compared with the neat ME compound (Table 1), which has been interpreted by Wankhede et al. [27] as the effect of a decrease in the bond order due to ME chemisorption on the surface of NP.

In the case of PVP–CdSe NP (Fig. 1c) the absorption peak at 1682 cm^{-1} can be assigned to C=O stretching band and those in the region of 1500–1200 cm^{-1} to C–H or C–N motions. The variation in the width of C=O stretching band confirmed the interaction between PVP and Cd^{2+}. This width variation is due to adsorption of CdSe NP on the surface of PVP which prevents the self association of lactam [29].

UV–Vis absorbance

UV–Vis absorption spectra were used to study the size of NP as a function of different synthesis parameters because the absorption edge shifted with size due to the quantum size effect. The size of NP was obtained from the peak positions. One can estimate the average size of CdSe NP by Eq. (1) [30].

$$D = \left(1.6122 \times 10^{-9}\right)\lambda^4 - \left(2.6575 \times 10^{-6}\right)\lambda^3 + \left(1.6242 \times 10^{-3}\right)\lambda^2 - (0.4277)\lambda + (41.57) \quad (1)$$

where D is the average diameter of CdSe NP and λ is the wavelength of the absorption peak. The value of the absorption peak was chose at the point where the absorption band curve reaches a maximum in every sample as this is considered as the mean particle size of the sample. The diameter of CdSe NP ranged from 1.2 to 3 nm. The estimated

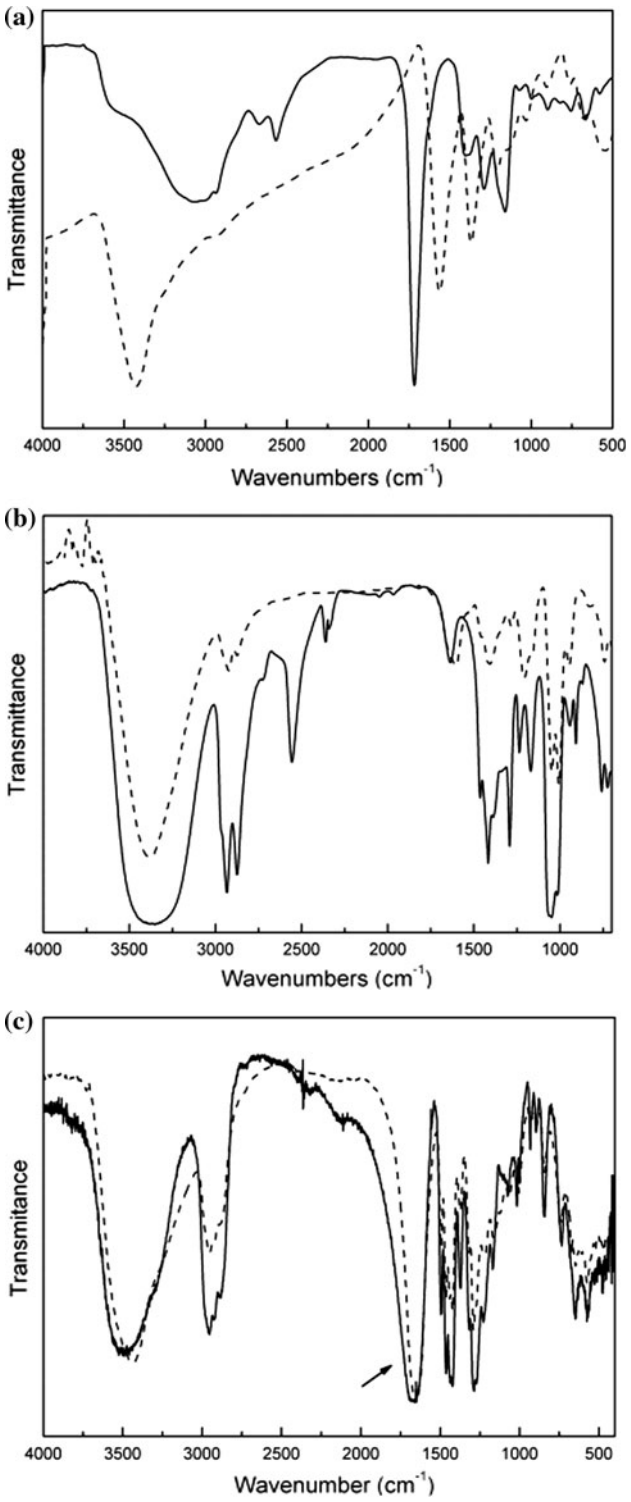

Fig. 1 FTIR spectra of: **a** neat ThGA (*solid lines*) and ThGA–CdSe (*dashed lines*), **b** neat ME (*solid lines*) and ME–CdSe (*dashed lines*) and **c** neat PVP (*solid lines*) and PVP–CdSe (*dashed lines*)

Table 1 FTIR analysis of ME and ME–CdSe nanoparticles

Type of vibrations	Mercaptoethanol (cm^{-1})	CdSe–ME (cm^{-1})
C–H stretching, asymm CH_2	2935, 2880	2922, 2870
O–H deformation	1419	1412
CH_2 wagging	1295, 1175	1282, 1162
C–O primary stretching	1055	1045

results are shown in Table 2. These given nanoparticle sizes are only orientative to obtain the trend of nanoparticle size changes with different synthesis parameters as this technique do not provide the needed level of accuracy for such small sizes.

pH effect

ThGA and ME-stabilized CdSe NP were synthesized by means different pH values prior to addition of Na_2SeSO_3 aqueous solution to Cd–thiolate complex solution. 7, 9 and 11 were the pH values used in the synthesis reaction. As can be seen in Fig. 2, in the case of ThGA-stabilized NP, the exciton peak wavelength shifted to the red region distinctly from previous work where the exciton peak wavelength decreased as the pH value increased [17]. An explanation to this size variation behaviour could be that at higher pH conditions due to high concentration of OH^- groups, conversion of $SeSO_3^{2-}$ to HSe^- was more favoured, thus achieving an increase of Se^{-2} concentration in the synthesis solution [31].

$$Na_2SeSO_3 + OH^- \rightarrow Na_2SO_4 + HSe^-$$

During CdSe nanoparticle synthesis, a competition between ThGA and HSe^- anions for Cd^{2+} binding sites occurred. As the concentration of Se^{-2} increased in the solution, the probability of Se^{-2} ions to bind with Cd^{2+} ions increased. Therefore, the NP continued growing upon pH and bigger-size NP were obtained, as shown in Fig. 2 [32].

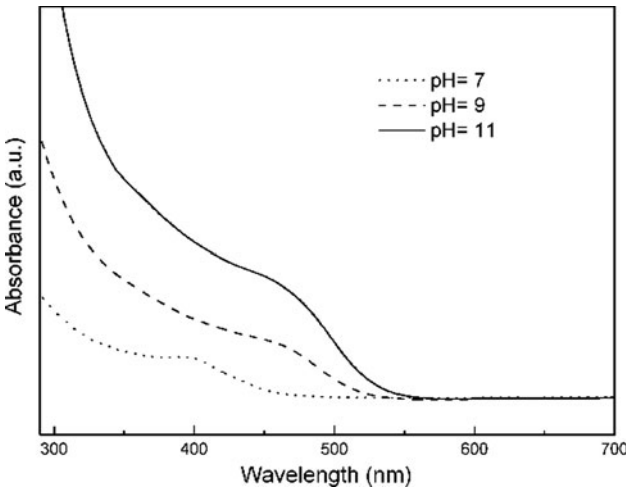

Fig. 2 UV–Vis absorption spectra for different pH synthesized ThGA–CdSe nanoparticles: *a* pH = 7, *b* pH = 9 and *c* pH = 11

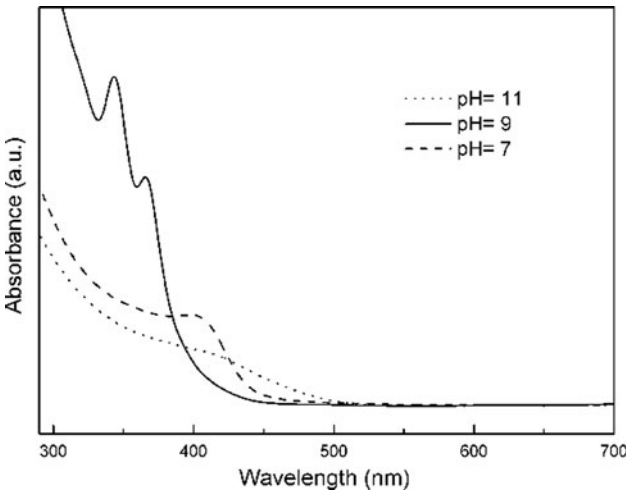

Fig. 3 UV–Vis absorption spectra for different pH synthesized ME–CdSe nanoparticles: *a* pH = 7, *b* pH = 9 and *c* pH = 11

On the other hand, the absorption spectra for ME–CdSe NP, Fig. 3 shows that the tendency of the nanoparticle size was to decrease as the pH increased from 7 to 9.

Table 2 Average diameter of CdSe nanoparticles determined from their UV–Vis absorbance spectra, XRD and TEM measurements

Sample	ThGA pH = 7	ThGA pH = 9	ThGA pH = 11	ThGA Cd:Se (5:1)	ME pH = 7	ME pH = 9	ME pH = 11	ME Cd:Se (1:1)	ME Cd:Se (5:1)	PVP Cd:Se (5:1)
Absorbance peak (nm)	391	451	459	366	399	365	384	400	298	543
Particle size (nm) UV–Vis	1.47	1.96	2.01	1.24	1.54	1.23	1.41	1.55	0.74	2.91
Particle size (nm) XRD	1.3	1.9	1.9	1.1	1.4	1.2	1.4	1.5		2.7
Particle size (nm) TEM	2–4 ± 0.7	2–4 ± 0.7	2–4 ± 0.7	2–3 ± 0.7	2–4 ± 0.7	2–4 ± 0.7	2–4 ± 0.7	2–4 ± 0.7		4–6 ± 0.7

Meanwhile, between pH 9 and 11, the nanoparticle size increased. The main difference between the two used mercapto stabilizing agents is the functional group. Whilst in ThGA there is an acid functional group (–COOH), in ME the hydroxyl group is neutral. This functional group could modulate the concentration of the Cd–thiol complex which plays a critical role in nanocrystal growth. As free Cd^{2+} only appears at pH lower than 2, Cd–thiol complex mediates CdSe nanoparticle synthesis. As hydroxyl group Cd–thiolate complex concentration behaviour has been shown to be similar to size variation in the same conditions [33], nanoparticle size varied with concentration of Cd–thiolate complex.

Cd/Se ratio effect

Five (Cd)/(Se) ratios (1/5, 1/2, 1/1, 2/1 and 5/1) were used. In all the cases, the (Cd)/(stabilizing agent0 ratio was kept constant (1/2 in the case of mercapto groups and 0.5 mM for PVP). Figure 4 shows absorbance spectra for different Cd/Se ratios using ThGA as stabilizing agent. In the case of 1/5, 1/2 and 1/1 ratios an insoluble precipitate with bulk spectral properties was achieved. The solutions were centrifuged to ensure there was no particle in suspension. As Cd:Se ratio decreased the particle size increased. As stated above, as the number of HSe^{-} anions increased so did the probability of finding Se^{-2} at the nanoparticle surface. This fact decreased the possibility to terminate or stabilize nanocrystal surfaces by ThGA.

Figure 5 spectra show a similar behaviour for ME–CdSe NP in the case of 1/5, 1/2, 2/1 and 5/1 ratios. Whilst insoluble precipitant was obtained for ThGA-capped NP at 1/1 Cd:Se ratio, a good suspension was obtained in the case of ME stabilizing agent. Nevertheless, the particles were precipitated after a few days. For 5/1 ratio, particles exhibited significantly blue shifted absorbance below 300 nm from 716 nm of the bulk CdSe band gap. Nosaka et al. [32] proposed that this absorbance wavelength indicates the formation of relatively stable clusters which may become a crystalline structure for constructing CdSe NP.

As seen in the absorbance spectra in Fig. 6 for PVP–CdSe NP, the only stable suspension was achieved for Cd:Se 5/1 ratio. For the other ratios insoluble precipitates were obtained. Besides the effect of the competition between HSe^{-} and PVP for Cd^{2+} binding molecules, it was seen that a minimum PVP concentration bigger than the needed one for mercapto compounds was needed to obtain an effective capping of the particles. Even when Cd:Se ratio was 2, a precipitate was obtained in a dissimilar way to thiol-capped

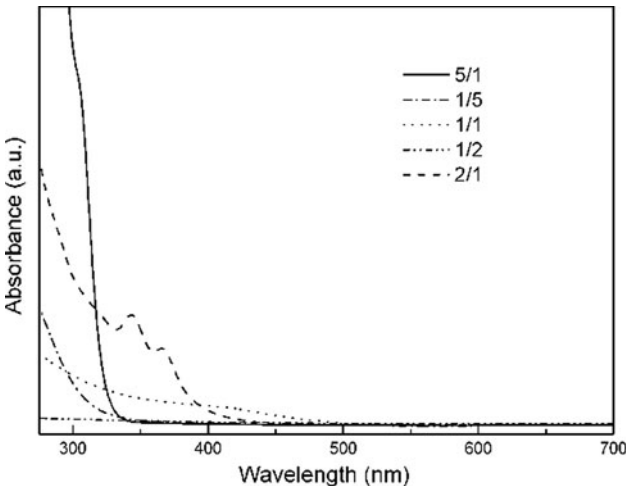

Fig. 5 UV–Vis absorption spectra for different Cd:Se ratio synthesized ME–CdSe nanoparticles: *a* 1:5, *b* 1:2, *c* 1:1, *d* 2:1 and *e* 5:1

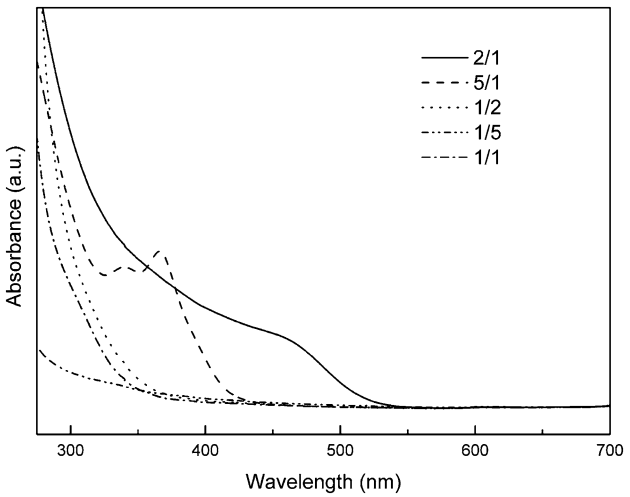

Fig. 4 UV–Vis absorption spectra for different Cd:Se ratio synthesized ThGA–CdSe nanoparticles: *a* 1:5, *b* 1:2, *c*1:1, *d* 2:1 and *e* 5:1

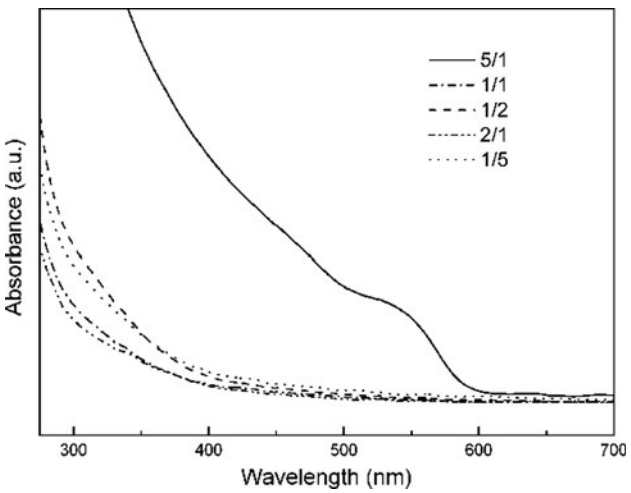

Fig. 6 UV–Vis absorption spectra for different Cd:Se ratio synthesized PVP–CdSe nanoparticles: *a* 1:5, *b* 1:2, *c* 1:1, *d* 2:1 and *e* 5:1

NP. These differences can be attributed to the different interactions between the thiol group and PVP with Cd^{2+} ions in the process of formation of the particles [34].

Ligand effect

Three different ligands were used as stabilizing agents to study their effect on the particle size. On one hand, two mercapto compounds (ThGA and ME) were used to study the influence of the functional group; on the other hand, poly(vinyl pyrrolidone) was used to analyze the different effect of chemical binding and physical binding on the size of NP. The Cd/Se ratio was 2/1 in the three cases and the used pH was 9. A bigger amount of PVP was used in this synthesis compared with the study of Cd/Se ratio due to results in these previous synthesis parameters where it was seen that a minimum amount of PVP was needed to obtain stable suspensions. Very stable suspensions were achieved in all the cases. As shown in Fig. 7, larger particles were formed when PVP was used as stabilizing agent due to the bigger size of the molecule of PVP compared to mercapto compounds. This larger size of the molecule could result in a worse covering of CdSe particles, which would facilitate the formation of larger particles. Regarding the effect of the functional group of mercapto compound stabilizing agent on nanoparticle size, ME–CdSe particles were smaller than ThGA–CdSe ones. The different functional group of the capping agent can be the reason for this size variation. In addition to the different pK_{sh} (pK_a for the SH group of the thiol group) of the thiol groups, which affect

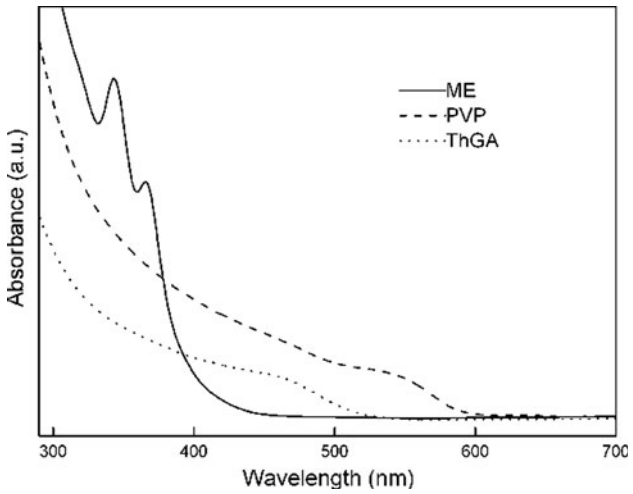

Fig. 7 UV–Vis absorption spectra for different capping agent synthesized CdSe nanoparticles: *a* ThGA, *b* ME and *c* PVP

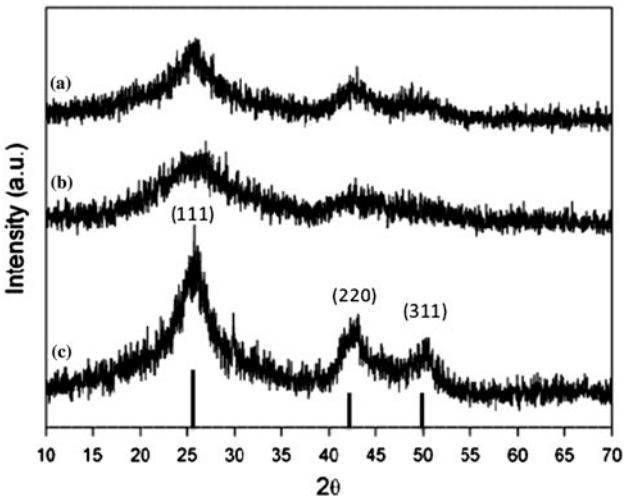

Fig. 8 X-ray powder diffractogram of different capping agent synthesized CdSe nanoparticles: *a* ThGA, *b* ME and *c* PVP

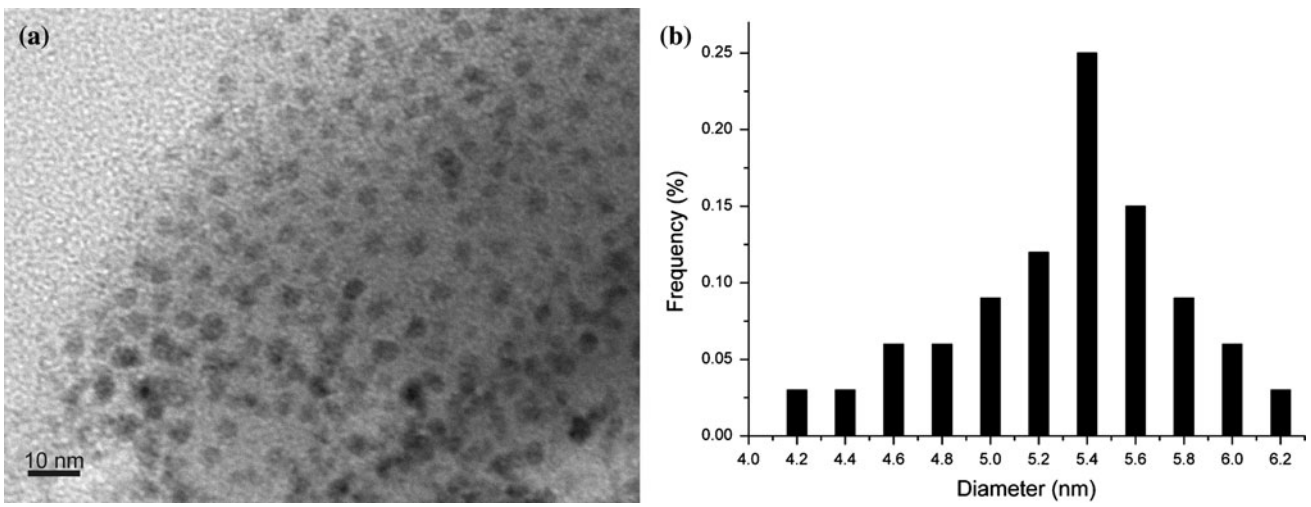

Fig. 9 TEM image of PVP–CdSe nanoparticles (**a**) and particle size distribution of the sample (**b**)

the concentration of thiolate–Cd complex, the non-ionic characteristic of the OH group in ME molecules might accelerate the stabilization of the complex, thus allowing to achieve smaller particles [32].

XRD

The characteristic X-ray diffractograms of CdSe NP with the different stabilizing agents are shown in Fig. 8. The broad peaks imply that the nanoparticle sizes were very small. The diffractogram patterns confirmed the crystalline cubic structure of CdSe NP. Diffraction peaks at around 25.6°, 42.2° and 50.0° correspond to (111), (220) and (311) planes of cubic type CdSe. Cubic structure has been found to be more preferable for thiol-capped CdSe NP [23], as opposed to the hexagonal phase for TOPO/TOP technique obtained ones [35]. The average nanoparticle sizes were obtained from the full width at half-maximum intensity of the most intense peak by means of Scherrer formula [36], as shown by Eq. (2).

$$D = 0.9\lambda/\beta\cos\theta \quad (2)$$

where β is the full width at half maximum, λ is the wavelength of X-ray used and θ is the Bragg's angle. As in the UV–Vis measurements, the given nanoparticle sizes in Table 2 are only orientative. As shown in Table 2, the variation of NP size was in good agreement with the obtained ones from UV–Vis measurements.

TEM measurements

TEM measurements were made also to obtain the size of the NP. Although the average sizes estimated from TEM micrographs, see Table 2, were generally larger, the trends of size variations with the synthesis parameters maintained similar to the previous ones. Figure 9a shows a typical TEM overview micrograph of CdSe NP stabilized by PVP. Figure 9b shows the distribution of the CdSe NP sizes which the most of them are in the range of 4 and 6 nm. 75 NP were taken to obtain an average value.

Conclusions

The effects of different aqueous synthesis parameters in the size of CdSe NP were studied. pH, Cd/Se ratio and different types of stabilizing agents were analyzed. The different parameters are not independent from each other. A close relationship was set between them, where a change in one of the parameters affected on the other ones. pH effects were different depending on the functional group of the mercapto compound, whilst at the same pH, smaller particles were obtained with ME stabilizing agent. Smaller size NP were obtained with mercapto compounds than when PVP was used as stabilizing agent due to a better capping of the surface and the chemical nature of the binding. A higher minimum concentration needed for PVP to reach a good covering of the particles to avoid aggregation and obtain a stable suspension was observed. In the case of the Cd:Se ratio, a similar trend was obtained for different pH and stabilizing agents at different Cd:Se ratios as for all the samples size increased as Cd:Se ratio decreased.

Acknowledgements Financial support is gratefully acknowledged from the Basque Country Government in the frame of Grupos Consolidados (IT-365-07), ETORTEK/inanoGUNE (IE09-243), ETORTEK/nanoIKER (IE11-304) and SAIOTEK 2010 (S-PE10UN40) projects and the Spanish Ministry of Education and Science for MAT2009-06331 project. The authors also thank the technical and human support provided by SGIker (UPV/EHU, MICINN, GV/EJ, ERDF and ESF). In memoriam of Dr. Iñaki Mondragon Egaña.

References

1. Henglein A (1989) Chem Rev 89:1861
2. Ouyang J, Chang M, Li X (2012) J Mater Sci 47:4187. doi: 10.1007/s10853-012-6273-x
3. Weiss EA, Chiechi RC, Geyer SM, Porter VJ, Bell DC, Bawendi MG, Whitesides GM (2008) J Am Chem Soc 130:74
4. Klimov VI (2007) Annu Rev Phys Chem 58:635
5. Chen X, Hutchison JL, Dobson PJ, Wakefield G (2008) J Colloid Interface Sci 319:140
6. Rogach AL, Nicholas AK, Dimitry SK, Susha SA, Caruso F (2002) Colloids Surf A Physicochem Eng Asp 202:135
7. Alivisatos AP (1996) J Phys Chem 100:13226
8. Murray CB, Norris DJ, Bawendi MG (1993) J Am Chem Soc 115:8706
9. Katari JEB, Colvin V, Alivisatos AP (1994) J Phys Chem 98:4109
10. Peng ZA, Peng X (2001) J Am Chem Soc 123:183
11. Talapin DV, Rogach AL, Kornowsky A, Haase M, Weller H (2001) Nano Lett 1:207
12. Talapin DV, Haubold S, Rogach AL, Kornowski A, Haase M, Weller H (2001) J Phys Chem B 105:2260
13. Qu L, Peng ZA, Peng X (2001) Nano Lett 1:333
14. Qu L, Peng X (2002) J Am Chem Soc 124:2049
15. Micic OI, Curtis CJ, Jones KM, Sprague JR, Nozik AJ (1994) J Phys Chem 98:4966
16. Cao YW, Banin U (2000) J Am Chem Soc 122:9692
17. Spanhel L, Haase M, Weller H, Henglein A (1987) J Am Chem Soc 109:5649
18. Vossmeyer T, Katsikas L, Giersig M, Popovic IG, Giesner K, Chemseddine A, Eychmüller A, Weller H (1994) J Phys Chem 98:7665
19. Rogach AL, Katsikas L, Kornowski A, Su D, Eychmüller A, Weller H (1996) Ber Bunsenges Phys Chem 100:1772
20. Rogach AL, Katsikas L, Kornowski A, Gao M, Eychmüller A, Weller H (1999) J Phys Chem B 103:3065

21. Yuan Z, Ma Q, Zhang A, Cao Y, Yang J, Yang P (2012) J Mater Sci 47:3770. doi:10.1007/s10853-011-6228-7
22. Harrison MT, Kershaw SV, Burt MG, Eychmüller A, Weller H, Rogach AL (2000) Mater Sci Eng B 69:355
23. Chen X, Hutchison JL, Dobson PJ, Wakefield G (2009) J Mater Sci 44:285. doi:10.1007/s10853-008-3055-6
24. Gaponik N, Talapin DV, Rogach AL, Hoppe K, Shevchenko EV, Kornowski A, Eychmüller A, Weller H (2002) J Phys Chem B 106:7177
25. Rietveld HM (1969) J Appl Crystallogr 2:65
26. Rodriguez-Carvajal (1993) J Phys B 192:55
27. Wankhede ME, Inamdar SN, Deshpande A, Thete AR, Pasricha R, Kulkarni SK, Haram SK (2008) Bull Mater Sci 31:291
28. Tang H, Yan M, Zhang H, Xia M, Yang D (2005) Mater Lett 59:1024
29. Yao H, Takahara S, Mizuma H, Kozeki T, Hayashi T (1996) Jpn J Appl Phys 35:4633
30. Nguyen HQ (2010) Adv Nat Sci Nanosci Nanotechnol. 1. doi:10.1088/2043-6254/1/2/025004
31. Yochelis S, Hodes G (2004) Chem Mater 16:2740
32. Nosaka Y, Ohta N, Fukuyama T, Fujii N (1993) J Colloid Interface Sci 155:23
33. Winter JO, Gomez N, Gatzert S, Schmidt CE, Korgel BA (2005) Colloid Surf A Physicochem Eng Asp 254:147
34. Saraswathi Amma B, Ramakrishna K, Pattabi M (2007) J Mater Sci Mater Electron 18:1109
35. Siy JT, Brauser EM, Bartl MH (2011) Chem Commun 47:364
36. Shyju TS, Anandhi S, Indirajith R, Gopalakrishnan R (2010) J Alloy Compd 506:892